Oscillatory Magnetostriction in Multivalley Semiconductors: Application to p-Type PbTe

Henry S. Belson* and J. Richard Burke*
U. S. Naval Ordnance Laboratory, White Oak, Silver Spring, Maryland 20910
and
Earl Callen†
Department of Physics, American University, Washington, D. C.
(Received 11 September 1969; revised manuscript received 12 November 1970)

Magnetostriction oscillations of de Haas–van Alphen origin are observed in p-type PbTe, a single-band multivalley semiconductor. The hole concentration of the material studied is 3×10^{18} cm^{-3}. The amplitude of the oscillations is related not only to the usual shear deformation potential Ξ_u, which causes intervalley charge transfer as the valleys rigidly shift relative to each other in energy, but also to six strain masses, which describe rotations and distortions of the hole valleys.

I. INTRODUCTION

The magnetrostriction of diamagnetic materials was extensively investigated many years ago by Kapitza.[1] Part of the renewed interest in this area during the last three years or so is a consequence of the feasibility of observing de-Haas–van-Alphen-type oscillations in the magnetostriction. As is well known, the de Haas–van Alphen oscillations in the magnetic susceptibility are the result of periodic variations in the free energy in high magnetic fields.[2] The oscillation in the magnetostriction is the response of the crystal to these variations as it strains to minimize the free energy.

The period of the magnetostriction oscillation is easily shown to be the same as that of the de Haas–van Alphen oscillation. Thus, a study of the dependence of this period on the crystallographic orientation of the magnetic field can be used to determine the shape of the Fermi surface. In this paper, however, we will be concerned primarily with the orientational dependence of the amplitude rather than the period of the oscillations. For the case of PbTe, the latter has been investigated in other experiments in more detail.[3,4]

The amplitudes of the magnetostriction oscillations are related to strain dependences of the energy and shape of the Fermi surface. For a Fermi surface consisting of ellipsoids of revolution, there are six phenomenological constants, which we call strain masses, that describe the strain dependence of the Fermi-surface shape. These six constants plus the shear deformation potential can be determined, at least in principle, by appropriate choice of the crystallographic orientation of the magnetic field and the direction in which the strain is measured.

The existence of magnetostriction oscillations of de Haas–van Alphen origin was first discussed by Chandrasekhar[5] and observed in bismuth by Green and Chandrasekhar.[6] Such oscillations were next reported on for beryllium[7] and zinc.[8] The first observation of the effect in a semiconductor was on n-GaSb, by Chandrasekhar, Condon, Fawcett, and Becker,[9] who stressed the importance of the amplitudes of the magnetostriction and de Haas–van Alphen oscillations; these authors determined the change in extremal cross section with strain. More recently, Mahajan and Sparlin[10] described magnetostriction in antimony. Aron, Chandrasekhar, and Thompson[11] were the first to report the observation of oscillations in PbTe, while preliminary accounts of the present work on this material have also been published.[12]

As is now well known, the Fermi surface of p-type PbTe consists of four prolate $\langle 111\rangle$ ellipsoids of revolution centered at the L points of the Brillouin zone.[13] The ellipsoids have a mass anisotropy of about 13 (Ref. 4) for a hole concentration of 3.0×10^{18} cm^{-3}, approximately the same as that of the samples investigated here. The multivalley nature of the valence band leads to magnetostriction effects which are large for a diamagnetic semiconductor. The dominant mechanism for magnetorstriction oscillations is the strain dependence of the L-point energies. When the magnetic field is in such a direction as to distinguish strongly between different ellipsoids, the free energy of the crystal is reduced by a shear strain which removes the degeneracy of the states at the L points and initiates an intervalley charge transfer. In high magnetic fields, the valleys "see-saw" in energy because of the periodicity of the free energy. This effect is describable by the usual deformation-potential theory.

When the magnetic field is in a $\langle 100\rangle$ direction, treating all valleys equally, rigid-band deformation potentials are of no avail, and crystal strains must

be ascribed almost entirely to rotations and distortions of the ellipsoids. These rotations and distortions are describable by six strain masses. These strain-masses are of three types: (i) The surfaces can remain ellipsoids of revolution, with the same orientations in momentum space, but with distorted longitudinal and transverse masses; (ii) the transverse cross section can be strained out-of-round; and (iii) the directions of the major axes of the ellipsoids can be rotated from the original $\langle 111 \rangle$ directions in k space.

The strain masses are calculable from a system of linear equations that relate the amplitudes of the strains, measured in several directions for several orientations of the magnetic field, to the strain masses and the shear deformation potential Ξ_u. The latter can be taken independently from piezoresistance measurements.[13] In practice, accurate values of the strain masses are difficult to obtain because of the large value of Ξ_u, alignment errors, and near cancellations of large terms in the system of simultaneous equations. A further complication arises from the need to evaluate or eliminate a de-Haas–van-Alphen-type factor in the theory. Therefore, we are unable to give numbers at this time. However, we will present the theory from which the strain masses can be obtained, show that they do make a finite contribution to magnetostriction in our samples, and give the amplitudes of the strain for a number of high-symmetry field and measurement directions.

II. THEORY

A. General

The oscillatory part of the free energy of a strained diamagnetic material in a magnetic field can be written

$$G = 2kT \sum_{s=1}^{\infty} \left(\frac{eB}{2\pi s c\hbar}\right)^{3/2} \sum_{\nu=1}^{d} \left(\left|\frac{\partial^2 S^{(\nu)}}{\partial k_B^2}\right|^{-1/2}\right) \Big/ \sinh\frac{2\pi^2 s k T}{\hbar\omega_c^{(\nu)}} \times \left(\exp\frac{-2\pi s}{\omega_c^{(\nu)}\tau}\right) \cos\left(\frac{sc\hbar}{eB} S^{(\nu)} - 2\pi s\gamma \pm \tfrac{1}{4}\pi\right) \times \cos\left(\frac{\pi}{2}\frac{m_c^{(\nu)} g^{(\nu)} s}{m_0}\right) + \frac{1}{2}\sum_{\mu,i} C^{\mu}(\epsilon_i^{\mu})^2 . \quad (2.1)$$

The first term on the right-hand side is the usual de Haas–van Alphen contribution[2] to the free energy of a material whose Fermi surface has d extremal cross sections $S^{(\nu)}$. The second term is the elastic energy expressed in terms of strains ϵ_i^{μ} defined below in Eq. (2.3). Since the highest populated Landau level carries the electrons of a particular valley to the Fermi surface, the free-energy contribution of that valley reaches a maximum, and the crystal strains in order to transfer electrons to other valleys and to lower-lying Landau levels. Thus magnetostriction is a Jahn-Teller distortion representing a compromise between a linear coupling of strain to electronic energy, and the quadratic elastic energy. The question arises as to which strain-dependent quantity in Eq. (2.1) is most responsible for the distortions, $|S^{(\nu)\prime\prime}|^{-1/2}$, $m_c^{(\nu)}$, $g^{(\nu)}$, or $S^{(\nu)}$. As we shall show, for our samples, the phase of the oscillations answers this question in favor of the last of these, the extremal cross section of the Fermi surface $S^{(\nu)}$ (Ref. 14).

Differentiating only $S^{(\nu)}$ in Eq. (2.1), and expanding for small strains, the minimum free energy is attained when

$$\epsilon_i^{\mu} = \frac{kT}{\pi C^{\mu}} \sum_{s=1}^{\infty} \left(\frac{eB}{2\pi s c\hbar}\right)^{1/2} \sum_{\nu=1}^{d} \left|\frac{\partial^2 S^{(\nu)}}{\partial k_B^2}\right|^{-1/2} \exp\left(\frac{-2\pi s}{\omega_c^{(\nu)}\tau}\right) \times \cos\left(\frac{\pi}{2}\frac{s g^{(\nu)} m_c^{(\nu)}}{m_0}\right) \Big/ \sinh\left(\frac{2\pi^2 s k T}{\hbar\omega_c^{(\nu)}}\right) \times \frac{\partial S^{(\nu)}}{\delta\epsilon_i^{\mu}} \sin\left(\frac{sc\hbar}{eB} S_0^{(\nu)} - 2\pi s\gamma \pm \tfrac{1}{4}\pi\right). \quad (2.2)$$

The strains ϵ_i^{μ} of Eq. (2.2) are basis functions (i) for irreducible representation (μ) of the cubic point group. They are convenient because, among other things, they diagonalize the elastic energy in Eq. (2.1). Referred to the cubic crystal axes, these strains are, explicitly,

$$\begin{aligned} \epsilon^{\alpha} &= \epsilon_{xx} + \epsilon_{yy} + \epsilon_{zz} , \\ \epsilon_1^{\gamma} &= (3^{1/2}/2)(\epsilon_{zz} - \tfrac{1}{3}\epsilon^{\alpha}) , \\ \epsilon_2^{\gamma} &= \tfrac{1}{2}(\epsilon_{xx} - \epsilon_{yy}) , \\ \epsilon_1^{\epsilon} &= \epsilon_{yz} , \\ \epsilon_2^{\epsilon} &= \epsilon_{zx} , \\ \epsilon_3^{\epsilon} &= \epsilon_{xy} , \end{aligned} \quad (2.3)$$

and the elastic constants associated with them are

$$\begin{aligned} C^{\alpha} &= \tfrac{1}{3}(C_{11} + 2C_{12}) , \\ C^{\gamma} &= 2(C_{11} - C_{12}) , \\ C^{\epsilon} &= 4C_{44} , \end{aligned} \quad (2.4)$$

where the C_{ij} are defined in terms of the engineering strains.

The prospect before us then is an evaluation of $\partial S^{(\nu)}/\partial\epsilon_i^{\mu}$ in Eq. (2.2) in terms of deformations of the hole ellipsoids.

B. Strain Dependence of $S^{(\nu)}$

When the angles between the principal axes (ξ, η, ζ) of an ellipsoid and the direction of the magnetic field have direction cosines α_{ξ}, α_{η}, and α_{ζ}, the extremal cross section of the νth ellipsoid can be written

$$S^{(\nu)} = 3^{2/3}\pi^{7/3} p^{(\nu)2/3} m_{\mathrm{gm}}^{1/2} / (m_{\xi}\alpha_{\xi}^2 + m_{\eta}\alpha_{\eta}^2 + m_{\zeta}\alpha_{\zeta}^2)^{1/2} , \quad (2.5)$$

where m_ξ, m_η, and m_ζ are the principal effective masses, m_{gm} is a geometric-mean mass defined by

$$m_{gm} = (m_\xi m_\eta m_\zeta)^{1/3} , \tag{2.6}$$

and $p^{(\nu)}$ is the hole concentration in the νth ellipsoid. For degenerate statistics and a parabolic band,

$$p_0^{(\nu)} = (\pi/3)\,(2m_{gm}\zeta^{(\nu)}/\pi^2\hbar^2)^{3/2} , \tag{2.7}$$

where $\zeta^{(\nu)}$ is the Fermi level relative to the extremum of the νth ellipsoid. The approximation of degenerate statistics is of course an accurate one at 4.2 °K. The assumption of a parabolic band is not completely adequate for PbTe, but it is made in order to simplify what is already a lengthy calculation.

In the unstrained crystal,

$$\begin{aligned} m_\xi^0 &= m_\eta^0 = m_t , \\ m_\zeta^0 &= m_l , \\ m_{gm}^0 &= (m_t^2 m_l)^{1/3} , \end{aligned} \tag{2.8}$$

and

$$p^{(\nu)} = (\pi/3)\,(2m_{gm}^0\zeta_0/\pi^2\hbar^2)^{3/2} . \tag{2.9}$$

m_t and m_l are, respectively, the effective masses transverse and parallel to a $\langle 111\rangle$ direction. The Fermi level ζ_0 is the same relative to the extremum of each valley, so that

$$p = 4p_0^{(\nu)} , \tag{2.10}$$

where p is the total hole concentration.

The energy of a hole ellipsoid transforms symmetrically under the group $D_{\infty h}$ (that of the homopolar diatomic molecule). Let us define sets of strains and of bilinear combinations of momentum components expressed in the local unstrained coordinate system (ξ, η, ζ) of a particular ellipsoid. These are

$$\begin{aligned} \epsilon_1 &= \mathrm{tr}\epsilon , \\ \epsilon_2 &= 3\epsilon_{\zeta\zeta} - \epsilon_1 , \\ \epsilon_3 &= \tfrac{1}{2}(\epsilon_{\xi\xi} - \epsilon_{\eta\eta}) , \\ \epsilon_4 &= \epsilon_{\eta\zeta} , \\ \epsilon_5 &= \epsilon_{\zeta\xi} , \\ \epsilon_6 &= \epsilon_{\xi\eta} , \end{aligned} \tag{2.11}$$

and

$$\begin{aligned} k_1 &= k^2 , \\ k_2 &= 3k_\zeta^2 - k^2 , \\ k_3 &= \tfrac{1}{2}(k_\xi^2 - k_\eta^2) , \\ k_4 &= k_\eta k_\zeta , \\ k_5 &= k_\zeta k_\xi , \\ k_6 &= k_\xi k_\eta . \end{aligned} \tag{2.12}$$

The energy of a strained ellipsoid is then

$$\begin{aligned} E(\vec{k}) = {} & (\Xi_d + \tfrac{1}{3}\Xi_u)\epsilon_1 + \tfrac{1}{3}\Xi_u\epsilon_2 + (\hbar^2/2m_1)k_1 + (\hbar^2/2m_2)k_2 \\ & + (\hbar^2/2\mu_{11})\epsilon_1 k_1 + (\hbar^2/2\mu_{12})\epsilon_1 k_2 \\ & + (\hbar^2/2\mu_{21})\epsilon_2 k_1 + (\hbar^2/2\mu_{22})\epsilon_2 k_2 \\ & + (\hbar^2/2\chi)(\epsilon_3 k_3 + \epsilon_6 k_6) + (\hbar^2/2\phi)(\epsilon_4 k_4 + \epsilon_5 k_5) . \end{aligned} \tag{2.13}$$

The deformation potentials $(\Xi_d + \frac{1}{3}\Xi_u)$ and $\frac{1}{3}\Xi_u$ are those defined by Herring and Vogt.[15] They represent rigid-band shifts in energy of the valley with strain. Terms in m are the unstrained energy. Terms in μ represent changes in longitudinal and transverse mass with local volume and local uniaxial strain. χ is a strain mass accompanying distortion of the constant-energy surface in the (ξ, η) plane from circular to elliptical. ϕ is a strain mass describing the rotation of the ellipsoid major axis away from the ζ direction with local shear strain.

Equation (2.5) for the extremal cross section shows that it can be considered to be a function of strain in three ways: (i) When the crystal strains, there can be a change in the number of charge carriers per unit volume $p^{(\nu)}$ in valley ν; (ii) since we keep terms in Eq. (2.13) only up to k^2, the ellipsoid remains an ellipsoid, but the principal masses can change from m_ξ, m_η, m_ζ to a new set m_ρ, m_σ, m_τ; and (iii) the direction cosines of the angles between the ellipsoid axes and the direction of the external field can change from α_ξ, α_η, α_ζ to α_ρ, α_σ, α_τ. For the strained ellipsoid, Eq. (2.5) is

$$S^{(\nu)}(\epsilon) = 3^{2/3}\pi^{7/3}p^{(\nu)2/3}m_{gm}^{1/2}/(m_\rho\alpha_\rho^2 + m_\sigma\alpha_\sigma^2 + m_\tau\alpha_\tau^2)^{1/2} , \tag{2.14}$$

which we must calculate to first order in ϵ, from Eq. (2.13).

First, let us calculate the second of the three contributions to $S^{(\nu)}(\epsilon)$, the change in principal masses. Substituting Eq. (2.12) into (2.13), we have

$$\begin{aligned} E(\vec{k}) = {} & (\Xi_d + \tfrac{1}{3}\Xi_u)\epsilon_1 + \tfrac{1}{3}\Xi_u\epsilon_2 + (\hbar^2/2m_\xi)k_\xi^2 \\ & + (\hbar^2/2m_\eta)k_\eta^2 + (\hbar^2/2m_\zeta)k_\zeta^2 + (\hbar^2\epsilon_6/2\chi)k_\xi k_\eta \\ & + (\hbar^2\epsilon_4/2\phi)k_\eta k_\zeta + (\hbar^2\epsilon_5/2\phi)k_\zeta k_\xi , \end{aligned} \tag{2.15}$$

with

$$\begin{aligned} 1/m_\xi \equiv {} & (1/m_1 - 1/m_2) + (1/\mu_{11} - 1/\mu_{12})\epsilon_1 \\ & + (1/\mu_{21} - 1/\mu_{22})\epsilon_2 + \epsilon_3/2\chi , \end{aligned} \tag{2.16}$$

$$\begin{aligned} 1/m_\eta \equiv {} & (1/m_1 - 1/m_2) + (1/\mu_{11} - 1/\mu_{12})\epsilon_1 \\ & + (1/\mu_{21} - 1/\mu_{22})\epsilon_2 - \epsilon_3/2\chi , \end{aligned} \tag{2.17}$$

$$\begin{aligned} 1/m_\zeta \equiv {} & (1/m_1 + 2/m_2) + (1/\mu_{11} + 2/\mu_{12})\epsilon_1 \\ & + (1/\mu_{21} + 2/\mu_{22})\epsilon_2 . \end{aligned} \tag{2.18}$$

Clearly,

$$m_\xi^0 = m_\eta^0 = (1/m_1 - 1/m_2)^{-1} = m_t \tag{2.19}$$

and

$$m_\xi^0 = (1/m_1 + 2/m_2)^{-1} = m_l \tag{2.20}$$

in the absence of strain. To first order in ϵ, the off-diagonal terms in Eq. (2.15) do not change the principal masses, but only rotate the axes:

$$m_\rho = m_\xi + O(\epsilon^2),\ m_\sigma = m_\eta + O(\epsilon^2),\ \text{and}\ m_\tau = m_\zeta + O(\epsilon^2)\ .$$

Inverting (2.16) to (2.18),

$$m_\rho = m_t\,[1 - m_t(1/\mu_{11} - 1/\mu_{12})\epsilon_1 - m_t(1/\mu_{21} - 1/\mu_{22})\epsilon_2 - m_t\epsilon_3/2\chi]\ , \tag{2.21}$$

$$m_\sigma = m_t\,[1 - m_t(1/\mu_{11} - 1/\mu_{12})\epsilon_1 - m_t(1/\mu_{21} - 1/\mu_{22})\epsilon_2 + m_t\epsilon_3/2\chi]\ , \tag{2.22}$$

$$m_\tau = m_l\,[1 - m_l(1/\mu_{11} + 2/\mu_{12})\epsilon_1 - m_l(1/\mu_{21} + 2/\mu_{22})\epsilon_2]\ , \tag{2.23}$$

and, with

$$m_{\rm gm}^0 = (m_t^2 m_e)^{1/3}\ , \tag{2.24}$$

$$m_{\rm gm} = m_{\rm gm}^0\{1 - \tfrac{1}{3}[(m_l + 2m_t)/\mu_{11} + 2(m_l - m_t)/\mu_{12}]\epsilon_1 - \tfrac{1}{3}[(m_l + 2m_t)/\mu_{21} + 2(m_l - m_t)/\mu_{22}]\epsilon_2\}\ . \tag{2.25}$$

Equations (2.21)–(2.25) describe the dependence of the effective masses on strain.

The third contribution to $S^{(\nu)}(\epsilon)$, the rotations of the principal ellipsoid axes, can also be calculated from Eq. (2.15). Diagonalizing the quadratic form to first order in ϵ, we obtain

$$\alpha_\rho = \alpha_\xi - \frac{m_t\epsilon_6}{4\chi}\,\alpha_\eta - \frac{\epsilon_5}{2(1/m_t + 1/m_l)\phi}\,\alpha_\zeta\ , \tag{2.26}$$

$$\alpha_\sigma = -\frac{m_t\epsilon_6}{4\chi}\,\alpha_\xi + \alpha_\eta - \frac{\epsilon_4}{2(1/m_t + 1/m_l)\phi}\,\alpha_\zeta\ , \tag{2.27}$$

and

$$\alpha_\tau = -\frac{\epsilon_5}{2(1/m_t + 1/m_l)\phi}\,\alpha_\xi - \frac{\epsilon_4}{2(1/m_t + 1/m_l)\phi}\,\alpha_\eta + \alpha_\zeta\ . \tag{2.28}$$

Equation (2.25) also describes part of the charge-transfer contribution to the strain dependence of $S^{(\nu)}(\epsilon)$ through the dependence of $p^{(\nu)}$ on $m_{\rm gm}$. Kosevich[16] discussed this effect in metals for the case of a uniform volume strain that produces a transfer of carriers from minor to major pieces of the Fermi surface. One possibility considered was complete depopulation of a small pocket. The situation in a single-band multivalley semiconductor is different because the volume strain merely shifts the Fermi level and the band extrema by the same amount with no effect on $p^{(\nu)}$. That is, the deformation potential $(\Xi_d + \frac{1}{3}\Xi_u)$ is immaterial to charge transfer, and to magnetostriction oscillations in a single-band material. However, under less symmetric strains, although the total number of carriers is still conserved, they are redistributed between the valleys, and this redistribution is governed by the second deformation potential Ξ_u. Because $\frac{1}{3}\Xi_u$ is the coefficient of ϵ_2, and as we shall see, the local axial strains ϵ_2 are combinations only of cubic shear strains ϵ_i^c, it is these shear strains that are excited by charge transfer, and that consequently have the largest amplitudes.

Under a general strain, then, the Fermi level relative to the extremum of the νth valley shifts by an amount $\delta\zeta$ different from that described by the change in $m_{\rm gm}$ alone. The new Fermi level is given by

$$\zeta^{(\nu)} = \zeta_0 + \delta\zeta^{(\nu)} - (\Xi_d + \tfrac{1}{3}\Xi_u)\epsilon_1^{(\nu)} - \tfrac{1}{3}\Xi_u\epsilon_2^{(\nu)}\ , \tag{2.29}$$

where $\delta\zeta^{(\nu)}$ is to be determined. Using Eqs. (2.25) and (2.29) and expanding, Eq. (2.7) then becomes

$$p^{(\nu)} = p_0^{(\nu)}\{1 + \tfrac{3}{2}\,\delta\zeta^{(\nu)}/\zeta_0 - \tfrac{1}{2}[3(\Xi_d + \tfrac{1}{3}\Xi_u)/\zeta_0 + (m_l + 2m_t)/\mu_{11} + 2(m_l - m_t)/\mu_{12}]\epsilon_1^{(\nu)} - \tfrac{1}{2}[\Xi_u/\zeta_0 + (m_l + 2m_t)/\mu_{21} + 2(m_l - m_t)/\mu_{22}]\epsilon_2^{(\nu)}\}\ . \tag{2.30}$$

To determine the Fermi-level shift, we note that the total density is

$$p = \textstyle\sum_\nu p^{(\nu)}\ , \tag{2.31}$$

and the total number of carriers is conserved. The latter is

$$V_0 p_0 = Vp\ , \tag{2.32}$$

which reduces to

$$4p_0^{(\nu)}(1 - \epsilon^\alpha) = \textstyle\sum_\nu p^{(\nu)}\ . \tag{2.33}$$

Making use of two relationships that are proved in the Appendix, i.e.,

$$\epsilon_1^{(\nu)} = \epsilon^\alpha \ \text{ for all } (\nu)$$

and

$$\textstyle\sum_\nu \epsilon_2^{(\nu)} = 0\ , \tag{2.34}$$

and of Eq. (2.29) $\delta\zeta$ can be substituted in Eq. (2.30), which eliminates $(\Xi_d + \frac{1}{3}\Xi_u)$, and we then have

$$p^{(\nu)} = p_0^{(\nu)}\{1 - \epsilon^\alpha - \tfrac{1}{2}[\Xi_u/\zeta_0 + (m_l + 2m_t)/\mu_{21} + 2(m_l - m_t)/\mu_{22}]\epsilon_2^{(\nu)}\}\ . \tag{2.35}$$

Equations (2.21)–(2.28) and Eq. (2.35) are the expressions necessary for the calculation of $S^{(\nu)}(\epsilon)$ in Eq. (2.14).

Substitution yields

$$S^{(\nu)} = S_0^{(\nu)}\{1 + [(m_l + 2m_t)/3\mu_{11} + 2(m_l - m_t)3\mu_{12} + (m_t^2/2f^{(\nu)})(1/\mu_{11} - 1/\mu_{12})(1 - \alpha_\xi^{(\nu)2})$$

$$+(m_l^2/2f^{(\nu)})(1/\mu_{11}+2/\mu_{12})\alpha_\xi^{(\nu)2}-\tfrac{2}{3}]\epsilon_1^{(\nu)}$$
$$+[\Xi_u/3\zeta_0+(m_t^2/2f^{(\nu)})(1/\mu_{21}-1/\mu_{22})(1-\alpha_\xi^{(\nu)2})+(m_l^2/2f^{(\nu)})(1/\mu_{21}+2/\mu_{22})\alpha_\xi^{(\nu)2}]\epsilon_2^{(\nu)}$$
$$+(m_t^2/4f^{(\nu)}\chi)(\alpha_\xi^{(\nu)2}-\alpha_\eta^{(\nu)2})\epsilon_3^{(\nu)}+(m_t^2/2f^{(\nu)}\chi)\alpha_\xi^{(\nu)}\alpha_\eta^{(\nu)}\epsilon_6^{(\nu)}$$
$$+(m_t m_l/2f^{(\nu)}\phi)(\alpha_\eta^{(\nu)}\alpha_\xi^{(\nu)}\epsilon_4^{(\nu)}+\alpha_\xi^{(\nu)}\alpha_\zeta^{(\nu)}\epsilon_5^{(\nu)})\}\ . \quad (2.36)$$

with

$$S_0^{(\nu)}=\frac{3^{2/3}\pi^{7/3}p_0^{(\nu)2/3}(m_{gm}^0)^{1/2}}{f^{(\nu)1/2}}$$
$$=\frac{3^{2/3}\pi^{7/3}p_0^{(\nu)2/3}K^{1/6}}{[1+(K-1)\alpha_\xi^{(\nu)2}]^{1/2}}\ , \quad (2.37)$$
$$f^{(\nu)}=m_t+(m_l-m_t)\alpha_\xi^{(\nu)2}\ ,$$

and

$$K=m_l/m_t\ .$$

The constant factor $-\frac{2}{3}$, in the amplitude of the volume strain $\epsilon_1^{(\nu)}$, is of purely geometric origin; the cross-sectional area change is two-thirds of the volume change. The minus sign comes from the volume change ϵ_1 being in real space, the cross-sectional area in reciprocal space. The effect of this density-of-states contribution is usually unimportant.

To calculate the strains ϵ_i^μ given by Eq. (2.2), we will want to differentiate Eq. (2.36) with respect to ϵ_i^μ. Therefore, we want to transform the local strains $\epsilon_i^{(\nu)}$, in which Eq. (2.36) is expressed and which are given by Eq. (2.11), to those of Eq. (2.3), which are expressed with respect to the cubic axes (x,y,z). These transformations, which are effected by the rotations

$$\overleftrightarrow{\epsilon}^{(\nu)}=\overleftrightarrow{\nu}\cdot\overleftrightarrow{\epsilon}\cdot\overleftrightarrow{\nu}^t\ , \quad (2.38)$$

are described in the Appendix. Using those results, the derivative $\partial S^{(\nu)}/\partial\epsilon_i^\mu$ needed for Eq. (2.2) can then be obtained from the relationship

$$\frac{\partial S^{(\nu)}}{\partial\epsilon_i^\mu}=\sum_j\frac{\partial S^{(\nu)}}{\partial\epsilon_j^{(\nu)}}\frac{\partial\epsilon_j^{(\nu)}}{\partial\epsilon_i^\mu}\ . \quad (2.39)$$

C. Magnetostriction Amplitude

The fractional change in length $\delta l/l$ in the direction $\vec{\beta}$ in a crystal sustaining Cartesian strains ϵ_{ij} is

$$\frac{\delta l}{l}=\sum_{i,j}\epsilon_{ij}\beta_i\beta_j\ . \quad (2.40)$$

The Cartesian strains ϵ_{ij} are found by inversion of the spherical tensors of Eq. (2.3), namely,

$$\epsilon_{xx}=\tfrac{1}{3}\epsilon^\alpha-\tfrac{1}{3}\sqrt{3}\,\epsilon_1^\gamma+\epsilon_2^\gamma\ ,$$
$$\epsilon_{yy}=\tfrac{1}{3}\epsilon^\alpha-\tfrac{1}{3}\sqrt{3}\,\epsilon_1^\gamma-\epsilon_2^\gamma\ ,$$
$$\epsilon_{zz}=\tfrac{1}{3}\epsilon^\alpha+\tfrac{2}{3}\sqrt{3}\,\epsilon_1^\gamma\ , \quad (2.41)$$
$$\epsilon_{yz}=\epsilon_1^\epsilon;\ \epsilon_{xz}=\epsilon_2^\epsilon;\ \epsilon_{xy}=\epsilon_3^\epsilon\ .$$

We now give some dilatations for three high-symmetry directions (α) of the magnetic field.

(a) $H\parallel[111]$:

$$(\delta l/l)_{[111]}=\tfrac{1}{3}\epsilon^\alpha_{[111]}+2\epsilon^\epsilon_{3\,[111]}\ , \quad (2.42a)$$
$$(\delta l/l)_{[1\bar{1}0]}=\tfrac{1}{3}\epsilon^\alpha_{[111]}-\tfrac{1}{3}\sqrt{3}\,\epsilon^\gamma_{1\,[111]}-\epsilon^\epsilon_{3\,[111]}\ . \quad (2.42b)$$

(b) $H\parallel[110]$:

$$(\delta l/l)_{[110]}=\tfrac{1}{3}\epsilon^\alpha_{[110]}-\tfrac{1}{3}\sqrt{3}\,\epsilon^\gamma_{1\,[110]}+\epsilon^\epsilon_{3\,[110]}\ , \quad (2.43a)$$
$$(\delta l/l)_{[1\bar{1}1]}=\tfrac{1}{3}\epsilon^\alpha_{[110]}+\tfrac{2}{3}(\epsilon^\epsilon_{2\,[110]}-\epsilon^\epsilon_{1\,[110]}-\epsilon^\epsilon_{3\,[110]}), \quad (2.43b)$$
$$(\delta l/l)_{[1\bar{1}0]}=\tfrac{1}{3}\epsilon^\alpha_{[110]}-\tfrac{1}{3}\sqrt{3}\,\epsilon^\gamma_{1\,[110]}-\epsilon^\epsilon_{3\,[110]}\ , \quad (2.43c)$$
$$(\delta l/l)_{[001]}=\tfrac{1}{3}\epsilon^\alpha_{[110]}+\tfrac{2}{3}\sqrt{3}\,\epsilon^\gamma_{1\,[110]}\ . \quad (2.43d)$$

(c) $H\parallel[001]$:

$$(\delta l/l)_{[001]}=\tfrac{1}{3}\epsilon^\alpha_{[001]}+\tfrac{2}{3}\sqrt{3}\,\epsilon^\gamma_{1\,[001]}\ , \quad (2.44a)$$
$$(\delta l/l)_{[100]}=\tfrac{1}{3}\epsilon^\alpha_{[001]}-\tfrac{1}{3}\sqrt{3}\,\epsilon^\gamma_{1\,[001]}\ . \quad (2.44b)$$

From a sufficient number of such measurements one should be able to obtain all six strain masses and the deformation potential Ξ_u. In principle, seven different measurements are not required, because in a general direction one should see four oscillations with different periods and amplitudes corresponding to four distinct extremal cross sections. However, in the measurements we have made, only a single period (plus its harmonics), corresponding to the smallest cross section, has been observed.

Chandrasekhar, Condon, Fawcett, and Becker[9] emphasized the desirability of performing simultaneous magnetostriction and de Haas–van Alphen measurements, so that those factors in the strain amplitude which also occur in the de Haas–van Alphen amplitude can be determined empirically from the latter measurements. Then the $\partial S^{(\nu)}/\partial\epsilon_i^\mu$ factors can be determined from the ratios of the amplitudes in the two measurements. However if one were able to observe oscillations of different periods from different valleys, or if one successively observed oscillations in sufficiently general directions $\vec{\beta}$ for a given field direction $\vec{\alpha}$, one could factor out the de Haas–van Alphen part of the amplitude in Eq. (2.2) without making other than magnetostriction measurements. In practice, we were not able to observe oscillations in enough general directions because our apparatus constrained us to special longitudinal and transverse orientations.

TABLE I. Theoretical magnetostriction amplitude factor $a_{[\alpha,\beta]}$ for field directions $[\alpha]$ and measurement directions $[\beta]$. The derivatives $\partial S/\partial\epsilon_i^\mu$ are to be evaluated for the field direction labeling the column in which they are located.

Measurement direction $[\beta]$	Field direction $[\alpha]$ [111]	[110]	[001]
[111]	$\frac{1}{3C^\alpha}\frac{\partial S}{\partial\epsilon^\alpha}+\frac{2}{C^\epsilon}\frac{\partial S}{\partial\epsilon_3^\epsilon}$ (Ref. 12)		
$[1\bar{1}0]$	$\frac{1}{3C^\alpha}\frac{\partial S}{\partial\epsilon^\alpha}-\frac{1}{\sqrt{3}\,C^\gamma}\frac{\partial S}{\partial\epsilon_1^\gamma}-\frac{1}{C^\epsilon}\frac{\partial S}{\partial\epsilon_3^\epsilon}$	$\frac{1}{3C^\alpha}\frac{\partial S}{\partial\epsilon^\alpha}-\frac{1}{\sqrt{3}\,C^\gamma}\frac{\partial S}{\partial\epsilon_1^\gamma}-\frac{1}{C^\epsilon}\frac{\partial S}{\partial\epsilon_3^\epsilon}$	$\frac{1}{3C^\alpha}\frac{\partial S}{\partial\alpha\epsilon^\alpha}-\frac{1}{\sqrt{3}\,C^\gamma}\frac{\partial S}{\partial\epsilon_1^\gamma}$
[110]		$\frac{1}{3C^\alpha}\frac{\partial S}{\partial\epsilon^\alpha}-\frac{1}{\sqrt{3}\,C^\gamma}\frac{\partial S}{\partial\epsilon_1^\gamma}+\frac{1}{C^\epsilon}\frac{\partial S}{\partial\epsilon_3^\epsilon}$	$\frac{1}{3C^\alpha}\frac{\partial S}{\partial\epsilon^\alpha}-\frac{1}{\sqrt{3}\,C^\gamma}\frac{\partial S}{\partial\epsilon_1^\gamma}$
$[1\bar{1}1]$		$\frac{1}{3C^\alpha}\frac{\partial S}{\partial\epsilon^\alpha}-\frac{2}{3C^\epsilon}\left(\frac{\partial S}{\partial\epsilon_3^\epsilon}+\frac{\partial S}{\partial\epsilon_1^\epsilon}-\frac{\partial S}{\partial\epsilon_2^\epsilon}\right)$	
[001]		$\frac{1}{3C^\alpha}\frac{\partial S}{\partial\epsilon^\alpha}+\frac{2}{\sqrt{3}\,C^\gamma}\frac{\partial S}{\partial\epsilon_1^\gamma}$	$\frac{1}{3C^\alpha}\frac{\partial S}{\partial\epsilon^\alpha}+\frac{2}{\sqrt{3}\,C^\gamma}\frac{\partial S}{\partial\epsilon_1^\gamma}$

Equations (2.42)–(2.44) require the evaluation of the strains in each of the three principal directions. As we mentioned above, in each such direction we have been able to observe only the oscillations corresponding to the ellipsoid having the smallest extremal cross section. This is the only term in the summation over ν in Eq. (2.2) that we shall retain henceforth. Following Ref. 12, we write the oscillatory magnetostriction as the product of a magnetostriction amplitude factor a and a de Haas–van Alphen factor b:

$$(\delta l/l)_{[\alpha,\beta]}=a_{[\alpha,\beta]}b_{[\alpha]}\sin[(c\hbar/eB)S_0-2\pi\gamma+\tfrac{1}{4}\pi]\,. \tag{2.45}$$

According to Eq. (2.2),

$$b_{[\alpha]}=N(kT/\pi)\left(\frac{eB}{2\pi c\hbar}\right)^{1/2}\left|\frac{\partial^2 S}{\partial k_B^2}\right|^{-1/2}\exp(-2\pi/\omega_c^{(\nu)}\tau)\times\sinh^{-1}\frac{2\pi^2kT}{\hbar\omega_c^{(\nu)}}\cos\left(\frac{\pi g^{(\nu)}m_c^{(\nu)}}{2m_0}\right)\,, \tag{2.46}$$

$(eB/2\pi c\hbar)^{-1}$ times the usual de Haas–van Alphen amplitude, and N is the appropriate number of ellipsoids with the same extremal cross section. $a_{[\alpha,\beta]}$ is a constant, for a given direction of field and measurement. $b_{[\alpha]}$ depends only on field direction, not measurement direction, and is a function of field strength. The magnetostriction amplitudes $a_{[\alpha,\beta]}$ corresponding to the dilatations described in Eqs. (2.42)–(2.44) are given in Table I. The rows are labeled by the measurement direction and the columns by the field direction. The derivatives $\partial S/\partial\epsilon_i^\mu$ are, of course, a function of the field direction. They are to be evaluated for the field direction labeling the column in which they are located.

The magnetostriction amplitude factors are next related to the fundamental quantities, the six strain masses and the deformation potential, by Eqs. (2.36), (2.37), and (2.39). Labeling the dominant cross section $S^{(1)}$, we have

$H\|[111]$:

$$\frac{\partial S^{(1)}}{\partial\epsilon^\alpha}=S_0^{(1)}\left[\frac{m_l+2m_t}{3\mu_{11}}+\frac{2}{3}\frac{(m_l-m_t)}{\mu_{12}}+\frac{m_l}{2}\left(\frac{1}{\mu_{11}}+\frac{2}{\mu_{12}}\right)-\frac{2}{3}\right]\,, \tag{2.47a}$$

$$\frac{\partial S^{(1)}}{\partial\epsilon_1^\gamma}=0\,, \tag{2.47b}$$

$$\frac{\partial S^{(1)}}{\partial\epsilon_3^\epsilon}=S_0^{(1)}\left[-\frac{\Xi_u}{3\zeta_0}+\frac{m_l}{2}\left(\frac{1}{\mu_{21}}+\frac{2}{\mu_{22}}\right)\right]\,. \tag{2.47c}$$

$H\|[110]$:

$$\frac{\partial S^{(1)}}{\partial\epsilon^\alpha}=S_0^{(1)}\left[\frac{m_l+2m_t}{3\mu_{11}}+\frac{2(m_l-m_t)}{3\mu_{12}}+\frac{m_t^2}{2(2m_l+m_t)}\left(\frac{1}{\mu_{11}}-\frac{1}{\mu_{12}}\right)+\frac{m_l^2}{(2m_l+m_t)}\left(\frac{1}{\mu_{11}}+\frac{2}{\mu_{12}}\right)-\frac{2}{3}\right]\,, \tag{2.47d}$$

$$\frac{\partial S^{(1)}}{\partial\epsilon_1^\gamma}=\tfrac{1}{3}\sqrt{3}\,S_0^{(1)}\left(\frac{m_t^2}{4(2m_l+m_t)\chi}-\frac{2m_tm_l}{(2m_l+m_t)\phi}\right)\,, \tag{2.47e}$$

$$\frac{\partial S^{(1)}}{\partial\epsilon_1^\epsilon}=S_0^{(1)}\left[-\frac{\Xi_u}{3\zeta_0}+\frac{m_t^2}{2(2m_l+m_t)}\left(\frac{1}{\mu_{21}}-\frac{1}{\mu_{22}}\right)+\frac{m_l^2}{(2m_l+m_t)}\left(\frac{1}{\mu_{21}}+\frac{2}{\mu_{22}}\right)-\frac{m_t^2}{24(2m_l+m_t)\chi}-\frac{m_tm_l}{6(2m_l+m_t)\phi}\right]\,, \tag{2.47f}$$

$$\frac{\partial S^{(1)}}{\partial\epsilon_2^\epsilon}=\frac{\partial S^{(1)}}{\partial\epsilon_1^\epsilon}\,, \tag{2.47g}$$

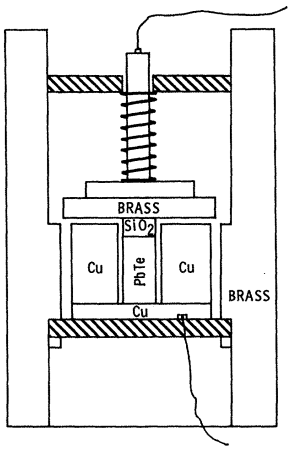

FIG. 1. Capacitance cell used for the measurements. The change in length of the PbTe sample changes the capacitance between the brass disk and the copper ring.

$$\frac{\partial S^{(1)}}{\partial \epsilon_3^{\epsilon}} = S_0^{(1)}\left[-\frac{\Xi_u}{3\xi_0} + \frac{m_t^2}{2(2m_l+m_t)}\left(\frac{1}{\mu_{21}} - \frac{1}{\mu_{22}}\right) + \frac{m_t^2}{(2m_l+m_t)}\left(\frac{1}{\mu_{21}} + \frac{2}{\mu_{22}}\right) + \frac{m_t^2}{12(2m_l+m_t)\chi} + \frac{m_t m_l}{3(2m_l+m_t)\phi}\right]. \quad (2.47h)$$

$H \| [001]$:

$$\frac{\partial S^{(1)}}{\partial \epsilon^{\alpha}} = S_0^{(1)}\left[\frac{m_l+2m_t}{3\mu_{11}} + \frac{2(m_l-m_t)}{3\mu_{12}} + \frac{m_t^2}{(m_l+2m_t)}\left(\frac{1}{\mu_{11}} - \frac{1}{\mu_{12}}\right) + \frac{m_l^2}{2(m_l+2m_t)}\left(\frac{1}{\mu_{11}} + \frac{2}{\mu_{12}}\right) - \frac{2}{3}\right], \quad (2.47i)$$

$$\frac{\partial S^{(1)}}{\partial \epsilon_1^{\gamma}} = \tfrac{1}{3}\sqrt{3}\, S_0^{(1)} \times\left(\frac{m_t}{2(m_l+2m_t)\chi} + \frac{2m_t m_l}{(m_l+2m_t)\phi}\right). \quad (2.47j)$$

This completes the theory. Measurement of $\delta l/l$ and evaluation of $b_{[\alpha]}$, either by a sufficient number of observations of $\delta l/l$ or by independent measurement, would allow determination of $a_{[\alpha,\beta]}$. From the period of oscillation one has $S_0^{(1)}$, and hence one could evaluate Ξ_u, μ_{ij}, χ, and ϕ in Eqs. (2.48) above. Note that in these equations the masses μ_{21} and μ_{22} occur in the combinations $(1/\mu_{21} + 2/\mu_{22})$ and $(1/\mu_{21} - 1/\mu_{22})$. Because of the large mass anisotropy, the coefficient of the latter term is negligibly small. Therefore, it will be difficult to determine the individual values of these masses.

III. EXPERIMENTAL

Changes in sample length were detected by a capacitive technique in which the length of the sample determines the capacitance of one arm of a capacitance bridge. A three-terminal General Radio unit (type 1615A) was used. It was driven at a frequency of 1 kHz by the same oscillator used to provide the reference signal for a Princeton Applied Research HR8 lock-in amplifier that measured the bridge unbalance. The output of this amplifier was used to drive the vertical axis of an x-y recorder, while a signal proportional to the magnetic field was applied to the horizontal axis. A continuous plot of the magnetic field dependence of the capacitance, and thus of the sample length, is then obtained by sweeping the magnetic field.

The details of the capacitance cell in which the samples were mounted is shown in Fig. 1. One plate of the capacitor is basically a copper cylinder with an axial hole closed at one end. The sample sits in this hole wearing an insulating SiO_2 cap which protrudes slightly above the end surface of the cylinder. A brass disk, spring loaded against this cap, forms the second plate of the capacitor. To obtain the largest capacitance, one wants to have these plates as close together as possible. We have been able to set their separation at about 0.01 cm at room temperature without encountering shorting effects due to foreign material or differential thermal contraction of the cell in going to 4.2 °K. With this separation, the capacitance of the cell is of the order of 50 pF at 4.2 °K. The General Radio bridge is setable to about 10^{-6} of this. For our samples, which were about 4 mm long in the direction in which length changes were detected, the minimum observable strain $\delta l/l$ was about 10^{-9}. This corresponds to a δl of about 0.1 Å and a change of capacitance of about 10^{-5} pF.

The samples studied were taken from single crystals of p-type PbTe grown by the Czochralski technique.[17] They had a hole concentration of about 3.0×10^{18} cm^{-3}. Measurements were made at the National Magnet Laboratory. A vertical solenoid provided longitudinal fields in excess of 100 kG, while transverse measurements were made in a 67-kG horizontal split solenoid. At the upper end of these field ranges, oscillations having amplitudes corresponding to strains as large as 10^{-7} were observed.

IV. EXPERIMENTAL RESULTS

Figure 2 shows the magnetostriction oscillations that appeared when both the measurement and field directions were parallel to [111]. These oscillations have the largest amplitudes because the deformation-potential contribution to the strain is a maximum. Except for the second-harmonic component, the data consist of a single frequency (1.17×10^5 G) corresponding to the smallest extremal cross section of the [111] ellipsoid.

Figure 3 shows the oscillations that were observed with $H \| [001]$. Again the data consist of a fundamental frequency (1.92×10^5 G) and its second

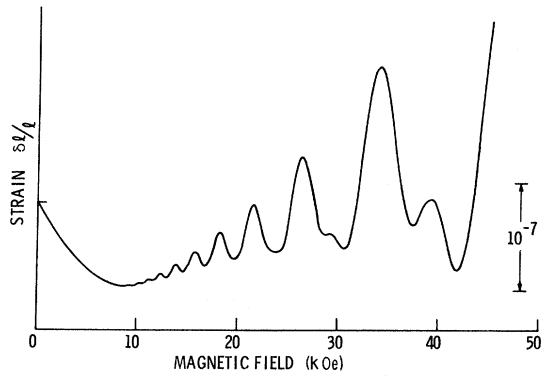

FIG. 2. Magnetostriction oscillations observed when both the measurement and field directions were parallel to [111]. Only the fundamental frequency and its harmonics, corresponding to smallest extremal cross section of the ellipsoids, are present.

harmonic. The amplitude of these oscillations is much smaller than those observed for $H\|[111]$ because the deformation-potential contribution is completely absent. A study of $\delta l/l$ over a range of field directions close to [001] showed a minimum value. This value is significantly larger than the contribution expected from the change in crystal density, and is direct evidence for the strain-mass contribution to the magnetostriction.

We assumed in our formulation of Eq. (2.2) that only the strain derivative of the extremal cross section $S^{(\nu)}$ in the cosine term of Eq. (2.1) need be considered. The validity of this assumption can best be tested by considering the phase of the oscillations. A knowledge of the phase is also necessary for determination of the sign of the magnetostriction coefficients $a_{[\alpha,\beta]}$ in Eq. (2.46). For this purpose, a more useful way to write this equation is

$$(\delta l/l)_{[\alpha,\beta]} = a_{[\alpha,\beta]} b_{[\alpha]} \sin(2\pi F/H - \phi_b - \phi_a) \,, \quad (4.1)$$

where $\phi_b = 2\pi\gamma \pm \frac{1}{4}\pi + \delta$ is the de Haas–van Alphen contribution to the phase, ϕ_a is the magnetostriction contribution, and $a_{[\alpha,\beta]}$ and $b_{[\alpha]}$ are considered to be positive numbers. For ellipsoidal surfaces, $+\frac{1}{4}\pi$ is appropriate, and for p-type PbTe with $p \simeq 3\times10^{18}$ cm^{-3}, it has been shown[4] that $\gamma \simeq \frac{1}{2}$ and $\delta = \pi$. The latter relationship is due to the term $\cos(\pi g^{(\nu)} m_c^{(\nu)}/2m_0)$ in Eq. (2.46) and the large value of $g^{(\nu)}$. Thus ϕ_a can be determined from the intercept at $1/H = 0$ of a plot of $(F/H - \phi_b/2\pi - \phi_a/2\pi)$ vs the $1/H$ values of the maxima and minima of $\delta l/l$. Figure 4 shows such a plot for two samples for which the measurement and field directions were parallel to [111]. The ordinate has been labeled for consistency with the previously determined[4] value of $\phi_b/2\pi = 1.30 \pm 0.05$. Using -1.75, the average of the intercepts of the two lines (which are identical within the experimental error in $1/H$), $\phi_a/2\pi = 0.45 \pm 0.05$. Thus it is reasonable to assume that there is a phase shift ϕ_a of exactly π due to a negative $a_{[\alpha,\beta]}$ for $\alpha = \beta = [111]$, and that Eq. (2.2) is very accurate for our samples.

The magnetic field dependence of the amplitudes of $\delta l/l$ for three orientations, in which the field and measurement directions are parallel, is shown in Fig. 5. These amplitudes were obtained from the envelopes of the oscillations for field ranges in which there was no apparent contribution from the second harmonic. In order to obtain magnetostriction amplitudes $a_{[\alpha,\beta]}$ from these data and Eq. (2.45), it is necessary to evaluate or eliminate the de Haas–van Alphen factor $b_{[\alpha]}$ given by Eq. (2.46). As was discussed in Sec. II, the evaluation can be obtained experimentally from an absolute measurement of de Haas–van Alphen amplitudes for the same sample, while elimination is possible if enough magnetostriction measurements are made. The former has not been carried out for our samples, while the latter was not possible because of constraints on our apparatus. We originally calculated values of $b_{[\alpha]}$ vs $1/H$ from parameters available in the literature and obtained $a_{[\alpha,\beta]}$ values by multiplying these calculations by the single constant that would result in agreement with $\delta l/l$ vs $1/H$. The curves in Fig. 5 were gotten in this manner. This is the least desirable method by which $a_{[\alpha,\beta]}$ can be obtained, but the values seemed reasonable. More extensive measurements as well as the availability of more accurate g values[4] for the hole concentration of our samples show that this procedure is too unreliable. This is especially true when trying to use the $a_{[\alpha,\beta]}$'s to calculate strain masses. However, for comparison with future work, we have constructed Table II, which gives amplitudes of $\delta l/l$ as a function of field and measurement direction for a single value of $1/H$.

V. SUMMARY AND CONCLUSIONS

We have derived expressions for the magnetostriction amplitude factor $a_{[\alpha,\beta]}$ of the magnetostriction oscillations $\delta l/l$ for field directions $[\alpha]$

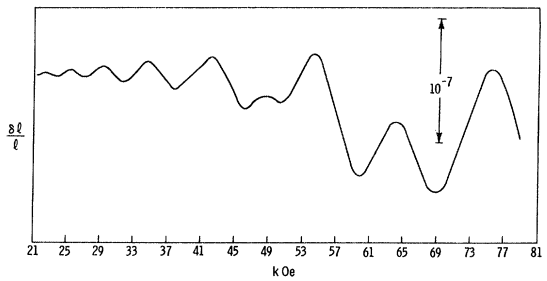

FIG. 3. Magnetostriction oscillations observed when both the measurement and field directions were parallel to [001]. Apparent deviations from the single frequency behavior expected for this field orientation are due to the presence of harmonics.

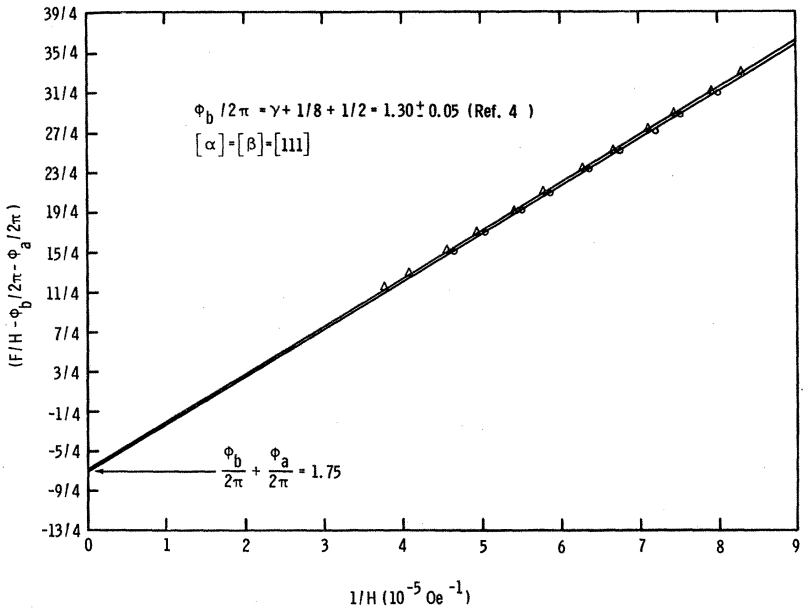

Fig. 4. Values of $(F/H - \phi_b/2\pi - \phi_a/2\pi)$, corresponding to extrema in $\delta l/l$, vs the $1/H$ values at which the extrema occur [see Eq. (4.1)]. Field and measurement directions were parallel to [111]. The two sets of data correspond to two sample having essentially the same hole concentration. The intercept at $1/H = 0$ determines ϕ_a, the phase shift of the magnetostriction oscillations relative to the phase of de Haas–van Alphen oscillations ϕ_b.

$\parallel$[111], [110], and [001], and for several measurement directions $[\beta]$ of high symmetry. This derivation has assumed that the principal contribution to the amplitude factor comes from the strain derivative of an extremal cross section of the Fermi surface. The phase of the oscillations shows this to be a good approximation for our p-type samples. These strain derivatives were then derived explicitly for an ellipsoid of revolution, multivalley model, in terms of the shear deformation potential Ξ_u and six strain masses. Ξ_u determines the strain that leads to intervalley charge transfer, while the strain

TABLE II. Amplitudes of the oscillatory strain $\delta l/l$ $\times 10^8$ for field directions $[\alpha]$, measurement directions $[\beta]$, and $1/H = 0.03$ kOe^{-1}. The numbers given are considered to be the most likely, while the true values should be within the ranges indicated. The numbers in parentheses are the frequencies of the fundamental oscillations for the field directions indicated.

Measurement direction $[\beta]$	Field direction $[\alpha]$ [111] (1.17×10^5 G)	[110] (1.39×10^5 G)	[001] (1.92×10^5 G)
[111]	7.9 ± 0.3		
[1$\bar{1}$0]	$5.0^{+0.5}_{-0.0}$	6.0 ± 0.3	$0.38^{+0.09}_{-0.01}$
[110]		$5.8^{+0.4}_{-0.1}$	
[1$\bar{1}$1]		$2.0^{+0.1}_{-0.2}$	
[001]		$0.33^{+0.01}_{-0.03}$	$0.80^{+0.10}_{-0.00}$
[100]			$0.32^{+0.04}_{-0.02}$

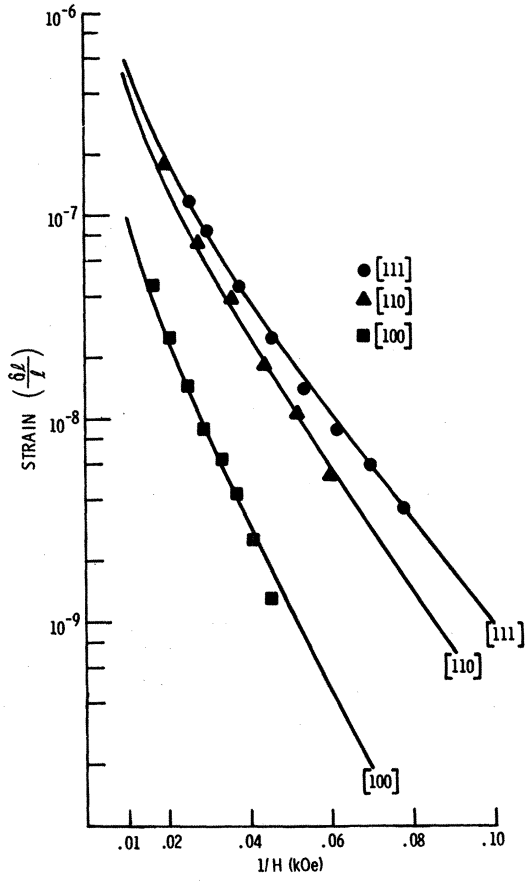

FIG. 5. Amplitudes of the oscillation at the fundamental frequency vs $1/H$ when both measurement and field directions were parallel to [111], [110], and [001].

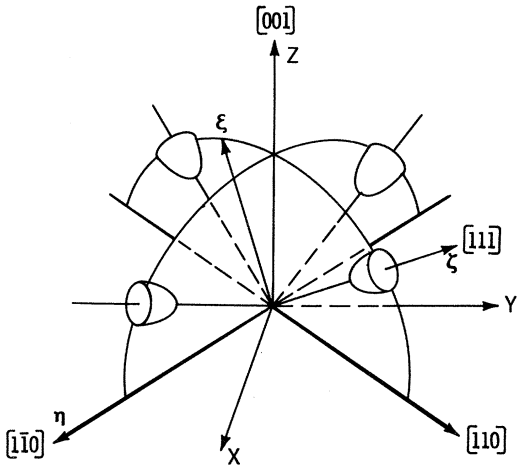

FIG. 6. Relationship of the principal axis system (ξ, η, ζ) of the [111] ellipsoid to the cubic axis system (x, y, z). (See Table III for the direction cosines of the principal axes of each ellipsoid.)

masses describe distortions and rotation of the ellipsoids.

The amplitude of the magnetostriction oscillations $\delta l/l$ is a product of the de Haas–van Alphen amplitude factor $b_{[\alpha]}$ and the magnetostriction amplitude factor $a_{[\alpha,\beta]}$. Evaluation of the latter requires either evaluation or elimination of the former. Because of the absence of de Haas–van Alphen measurements on our samples and the constraints on our apparatus, neither was possible experimentally. Calculations of $b_{[\alpha]}$ led to values of $a_{[\alpha,\beta]}$ that were too unreliable, especially for strain-mass calculations. As a consequence, only the amplitudes of the strain $\delta l/l$ are presented at this time. However these amplitudes clearly indicate that while the major contribution to the magnetostriction comes from the deformation potential, the strain-mass contribution is finite.

ACKNOWLEDGMENTS

We wish to acknowledge our collaboration with Dr. J. Babiskin and P. G. Siebenmann of the Naval Research Laboratory, and Dr. B. Houston and Dr. H. T. Savage of this laboratory in the early states of this work. We also wish to thank the National Magnet Laboratory, especially L. Rubin, for arranging the magnet time necessary for these experiments.

APPENDIX

We need to be able to transform from the strains expressed in the cubic axis system (x, y, z) to those in the principal axis system (ξ, η, ζ) of each of the four ellipsoids (see Fig. 6). The direction cosines of each of the four principal axis systems are given in Table III. Using these and the transformation equation (2.38), the following relationships are obtained:

$$\epsilon_1^{(\nu)} = \epsilon^{\alpha} \quad \text{(all } \nu\text{)}; \tag{A1}$$

$$\begin{aligned}
\epsilon_2^{(1)} &= \epsilon_1^{\epsilon} + \epsilon_2^{\epsilon} + \epsilon_3^{\epsilon}, \\
\epsilon_2^{(2)} &= \epsilon_1^{\epsilon} - \epsilon_2^{\epsilon} - \epsilon_3^{\epsilon}, \\
\epsilon_2^{(3)} &= -\epsilon_1^{\epsilon} - \epsilon_2^{\epsilon} + \epsilon_3^{\epsilon}, \\
\epsilon_2^{(4)} &= -\epsilon_1^{\epsilon} + \epsilon_2^{\epsilon} - \epsilon_3^{\epsilon};
\end{aligned} \tag{A2}$$

$$\begin{aligned}
\epsilon_3^{(1)} &= \tfrac{1}{3}\sqrt{3}\,\epsilon_1^{\gamma} - \tfrac{1}{6}\epsilon_1^{\epsilon} - \tfrac{1}{6}\epsilon_2^{\epsilon} + \tfrac{1}{3}\epsilon_3^{\epsilon}, \\
\epsilon_3^{(2)} &= \tfrac{1}{3}\sqrt{3}\,\epsilon_1^{\gamma} - \tfrac{1}{6}\epsilon_1^{\epsilon} + \tfrac{1}{6}\epsilon_2^{\epsilon} - \tfrac{1}{3}\epsilon_3^{\epsilon}, \\
\epsilon_3^{(3)} &= \tfrac{1}{3}\sqrt{3}\,\epsilon_1^{\gamma} + \tfrac{1}{6}\epsilon_1^{\epsilon} + \tfrac{1}{6}\epsilon_2^{\epsilon} + \tfrac{1}{3}\epsilon_3^{\epsilon}, \\
\epsilon_3^{(4)} &= \tfrac{1}{3}\sqrt{3}\,\epsilon_1^{\gamma} + \tfrac{1}{6}\epsilon_1^{\epsilon} - \tfrac{1}{6}\epsilon_2^{\epsilon} - \tfrac{1}{3}\epsilon_3^{\epsilon};
\end{aligned} \tag{A3}$$

$$\begin{aligned}
\epsilon_4^{(1)} &= 2(\tfrac{2}{3})^{1/2}\epsilon_2^{\gamma} - \tfrac{1}{6}(6)^{1/2}\epsilon_1^{\epsilon} + \tfrac{1}{6}(6)^{1/2}\epsilon_2^{\epsilon}, \\
\epsilon_4^{(2)} &= -2(\tfrac{2}{3})^{1/2}\epsilon_2^{\gamma} + \tfrac{1}{6}(6)^{1/2}\epsilon_1^{\epsilon} + \tfrac{1}{6}(6)^{1/2}\epsilon_2^{\epsilon}, \\
\epsilon_4^{(3)} &= 2(\tfrac{2}{3})^{1/2}\epsilon_2^{\gamma} + \tfrac{1}{6}(6)^{1/2}\epsilon_1^{\epsilon} - \tfrac{1}{6}(6)^{1/2}\epsilon_2^{\epsilon}, \\
\epsilon_4^{(4)} &= -2(\tfrac{2}{3})^{1/2}\epsilon_2^{\gamma} - \tfrac{1}{6}(6)^{1/2}\epsilon_1^{\epsilon} - \tfrac{1}{6}(6)^{1/2}\epsilon_2^{\epsilon};
\end{aligned} \tag{A4}$$

$$\begin{aligned}
\epsilon_5^{(1)} &= 2(\tfrac{2}{3})^{1/2}\epsilon_1^{\gamma} + \tfrac{1}{6}\sqrt{2}\,\epsilon_1^{\epsilon} + \tfrac{1}{6}\sqrt{2}\,\epsilon_2^{\epsilon} - \tfrac{1}{3}\sqrt{2}\,\epsilon_3^{\epsilon}, \\
\epsilon_5^{(2)} &= 2(\tfrac{2}{3})^{1/2}\epsilon_1^{\gamma} + \tfrac{1}{6}\sqrt{2}\,\epsilon_1^{\epsilon} - \tfrac{1}{6}\sqrt{2}\,\epsilon_2^{\epsilon} + \tfrac{1}{3}\sqrt{2}\,\epsilon_3^{\epsilon}, \\
\epsilon_5^{(3)} &= 2(\tfrac{2}{3})^{1/2}\epsilon_1^{\gamma} - \tfrac{1}{6}\sqrt{2}\,\epsilon_1^{\epsilon} - \tfrac{1}{6}\sqrt{2}\,\epsilon_2^{\epsilon} - \tfrac{1}{3}\sqrt{2}\,\epsilon_3^{\epsilon}, \\
\epsilon_5^{(4)} &= 2(\tfrac{2}{3})^{1/2}\epsilon_1^{\gamma} - \tfrac{1}{6}\sqrt{2}\,\epsilon_1^{\epsilon} + \tfrac{1}{6}\sqrt{2}\,\epsilon_2^{\epsilon} + \tfrac{1}{3}\sqrt{2}\,\epsilon_3^{\epsilon};
\end{aligned} \tag{A5}$$

$$\begin{aligned}
\epsilon_6^{(1)} &= -\tfrac{2}{3}\sqrt{3}\,\epsilon_2^{\gamma} - \tfrac{1}{3}\sqrt{3}\,\epsilon_1^{\epsilon} + \tfrac{1}{3}\sqrt{3}\,\epsilon_2^{\epsilon}, \\
\epsilon_6^{(2)} &= \tfrac{2}{3}\sqrt{3}\,\epsilon_2^{\gamma} + \tfrac{1}{3}\sqrt{3}\,\epsilon_1^{\epsilon} + \tfrac{1}{3}\sqrt{3}\,\epsilon_2^{\epsilon}, \\
\epsilon_6^{(3)} &= -\tfrac{2}{3}\sqrt{3}\,\epsilon_2^{\gamma} + \tfrac{1}{3}\sqrt{3}\,\epsilon_1^{\epsilon} - \tfrac{1}{3}\sqrt{3}\,\epsilon_2^{\epsilon}, \\
\epsilon_6^{(4)} &= \tfrac{2}{3}\sqrt{3}\,\epsilon_2^{\gamma} - \tfrac{1}{3}\sqrt{3}\,\epsilon_1^{\epsilon} - \tfrac{1}{3}\sqrt{3}\,\epsilon_2^{\epsilon}.
\end{aligned} \tag{A6}$$

Using these expressions, the derivatives $\partial S^{(\nu)}/\partial\epsilon_i^{\mu}$ of Eq. (2.39) can now be evaluated.

Equation (A1) was to be expected, as the scalar invariant is independent of coordinate system. This result was previously involved in Eq. (2.34). Summing $\epsilon_2^{(\nu)}$ over ν in Eq. (A2) produces the second result we invoked in Eq. (2.34). In fact,

$$\textstyle\sum_{\nu} \epsilon_1^{(\nu)} = 4\epsilon^{\alpha}, \tag{A7}$$

TABLE III. Direction cosines of the principal axes of each ellipsoid relative to the cubic axes. (See Fig. 6.)

ν	$\hat{\xi}$	$\hat{\eta}$	$\hat{\zeta}$
1	$\frac{1}{6}\sqrt{6}$ [1$\bar{1}$2]	$\frac{1}{2}\sqrt{2}$ [1$\bar{1}$0]	$\frac{1}{3}\sqrt{3}$ [111]
2	$\frac{1}{6}\sqrt{6}$ [112]	$\frac{1}{2}\sqrt{2}$ [110]	$\frac{1}{3}\sqrt{3}$ [$\bar{1}$11]
3	$\frac{1}{6}\sqrt{6}$ [112]	$\frac{1}{2}\sqrt{2}$ [$\bar{1}$10]	$\frac{1}{3}\sqrt{3}$ [1$\bar{1}$1]
4	$\frac{1}{6}\sqrt{6}$ [$\bar{1}$12]	$\frac{1}{2}\sqrt{2}$ [$\bar{1}\bar{1}$0]	$\frac{1}{2}\sqrt{3}$ [11$\bar{1}$]

$$\sum_\nu \epsilon_2^{(\nu)} = \sum_\nu \epsilon_4^{(\nu)} = \sum_\nu \epsilon_6^{(\nu)} = 0 \ , \qquad \text{(A8)}$$

and

$$\sum_\nu \epsilon_3^{(\nu)} = \tfrac{4}{3}\sqrt{3}\,\epsilon_1^\gamma \ , \qquad \text{(A9)}$$

$$\sum_\nu \epsilon_5^{(\nu)} = 8(\tfrac{2}{3})^{1/2}\epsilon_1^\gamma \ . \qquad \text{(A10)}$$

---

*Visiting Scientists, Francis Bitter National Magnet Laboratory, MIT, Cambridge, Mass.

†Supported in part at American University under NASA Grant No. NGR-09-003-014.

[1]P. Kapitza, Proc. Roy. Soc. (London) 131, 224 (1931); 135, 537 (1931).

[2]L. Landau, Z. Physik 64, 629 (1930). For a more recent discussion, see J. M. Ziman, *Principles of the Theory of Solids* (Cambridge U. P., Cambridge, England, 1964), p. 274

[3]K. F. Cuff, M. R. Ellett, and C. D. Kuglin, in *Proceedings of the International Conference on the Physics of Semiconductors, Exeter*, 1962 (The Institute of Physics and The Physical Society, London, England, 1962), p. 316.

[4]J. R. Burke, B. Houston, H. T. Savage, J. Babiskin, and P. G. Siebenmann, Bull. Am. Phys. Soc. 13, 484 (1968); J. R. Burke, B. Houston, and H. T. Savage, Phys. Rev. B 2, 1977 (1970).

[5]B. S. Chandrasekhar, Phys. Letters 6, 27 (1963).

[6]B. A. Green, Jr. and B. S. Chandrasekhar, Phys. Rev. Letters 11, 331 (1963).

[7]D. M. Sparlin, B. S. Chandrasekhar, and E. Fawcett, Bull. Am. Phys. Soc. 10, 350 (1965).

[8]L. Reitz and D. M. Sparlin, Bull. Am. Phys. Soc. 11, 169 (1966).

[9]B. S. Chandrasekhar, J. H. Condon, E. Fawcett, and W. M. Becker, Phys. Rev. Letters 17, 954 (1966).

[10]V. N. Mahajan and D. M. Sparlin, Bull. Am. Phys. Soc. 12, 286 (1967).

[11]P. R. Aron, B. S. Chandrasekhar, and T. E. Thompson, post-deadline paper, Chicago APS Meeting, 1967 (unpublished).

[12]H. S. Belson, J. R. Burke, E. Callen, B. Houston, H. T. Savage, J. Babiskin, and P. G. Siebenmann, Phys. Rev. Letters 19, 1428 (1967); Bull. Am. Phys. Soc. 12, 1119 (1967). In Eq. (4c) of the letter, $4C_{44}$ should be replaced by $2C_{44}$.

[13]For a recent review of work on PbTe, see J. R. Burke, Phys. Rev. 160, 636 (1967).

[14]Measurements by T. E. Thompson also confirm this.

[15]C. Herring and E. Vogt, Phys. Rev. 101, 944 (1956).

[16]A. M. Kosevich, Zh. Eksperim. i Teor. Fiz. 35, 249 (1958) [Sov. Phys. JETP 35, 171 (1959)].

[17]These crystals were kindly provided for us by B. Houston of this laboratory.

PHYSICAL REVIEW B VOLUME 3, NUMBER 12 15 JUNE 1971

Raman Study of the Semiconductor-Metal Transition in Ti_2O_3 †

A. Mooradian and P. M. Raccah

Lincoln Laboratory, Massachusetts Institute of Technology, Lexington, Massachusetts 02173

(Received 6 July 1970)

The Raman spectrum of Ti_2O_3 exhibits seven modes as predicted for the corundum structure. The persistence of all seven of these modes above the semiconductor-metal transition temperature indicates no space-group change on going through the phase transition. The A_{1g} mode at 269 cm^{-1} (300 °K) exhibits a significant frequency change (about 16%) and a large intensity increase relative to the other modes in the temperature range of the semiconductor-metal transition. These results are interpreted in terms of electronic and structural changes during the phase transition.

INTRODUCTION

Several physical properties of Ti_2O_3 undergo a rapid change over a range of 150 K° in the neighborhood of 400 °K. These include the lattice parameters,[1] the specific heat,[2] and the resistivity.[3] Below this range of temperature the material is a semiconductor and above this range the temperature dependence of the resistivity indicates metallic behavior.

We report here a study of the Raman-active modes, in frequency as well as in intensity, across the transition range. The study provides further information as to the nature of the change and agrees well with a previous model.

EXPERIMENTAL RESULTS

Surface Raman scattering was done using various (4579–5145-Å) excitation lines of an argon-ion laser. Single-crystal, oriented, and polished samples were used with the incident and scattered light propagat-